# ANALYSIS OF SHOCK WAVE PRESSURE IN TUNNELS WITH VARIABLE CROSS-SECTION USING ANSYS AUTODYN 3D SOFTWARE

PHÂN TÍCH GIÁ TRỊ ÁP SUẤT CỦA SÓNG XUNG KÍCH TRUYỀN TRONG ĐƯỜNG HẦM CÓ MẶT CẮT NGANG THAY ĐỔI BẰNG PHẦN MỀM ANSYS AUTODYN 3D

**NGO NGOC THUY**[a,*], **CAO CHU QUANG**[a], **VU NGOC ANH**[a]
*Military Technical Academy
*Tác giả đại diện: *Email*: ngongocthuyv2@gmail.com
*Ngày nhận 13/6/2025, Ngày sửa 26/6/2025, Chấp nhận 28/6/2025*
https://doi.org/10.59382/j-ibst.2025.vi.vol2-3

Abstract: *In the study of the effects of explosions, including bomb detonations, the analysis of shock wave propagation within tunnels is of critical importance. As shock waves traverse tunnel sections with varying cross-sectional geometries whether expanding or contracting the pressure distribution undergoes significant changes.*

*This paper systematically investigates the distribution of shock wave pressure in tunnels and regions with cross-sectional variations through numerical simulations conducted using ANSYS Autodyn 3D software. The obtained simulation results are compared with calculations derived from empirical formulas. Numerical analyses reveal that the discrepancy between the two approaches ranges from 3% to 33%, which is considered an acceptable margin of error in the study of shock wave propagation.*

Keywords: *shock wave, tunnel cross-section, cross-section changes, pressure value, Ansys Autodyn 3D.*

Tóm tắt: *Trong quá trình nghiên cứu tác động của bom hoặc các vụ nổ xảy ra, việc phân tích sự lan truyền của sóng xung kích trong đường hầm là điều hết sức cần thiết. Khi sóng xung kích di chuyển qua các đoạn đường hầm có sự thay đổi về mặt tiết diện, dù là mở rộng hay thu hẹp, giá trị áp suất của sóng sẽ biến đổi rõ rệt.*

*Bài báo này tập trung khảo sát sự phân bố áp suất của sóng xung kích lan truyền trong đường hầm và khu vực có biến đổi tiết diện, thông qua việc sử dụng phần mềm Ansys Autodyn 3D. Kết quả mô phỏng thu được sẽ được so sánh với kết quả tính toán theo công thức thực nghiệm. Các thử nghiệm số cho thấy sự chênh lệch giữa hai phương pháp nằm trong khoảng từ 3% đến 33%, một mức sai số có thể chấp nhận được trong nghiên cứu sự lan truyền sóng xung kích.*

Từ khóa: *sóng xung kích, mặt cắt ngang đường hầm, thay đổi mặt cắt, giá trị áp lực, Ansys Autodyn 3D.*

## 1. Introduction

Explosions within confined environments such as tunnels generate shock waves that present significant risks to both structural stability and human safety. Accurately understanding the behavior of these shock waves particularly as they travel through regions where the tunnel cross-section changes is essential for designing effective blast-resistant infrastructure. Changes in tunnel geometry, whether through expansion or contraction, can lead to substantial variations in pressure distribution, influencing how the structure responds to the blast load.

Regarding the determination of shock wave pressure values in regions with varying cross-sections, documents [1, 2, 3] have provided empirical formulas. However, for points at distances three times of tunnel diameter, where a diffraction zone of the wave appears, no existing documents have addressed this issue. Therefore, this paper focuses on utilizing the Ansys Autodyn software application to accurately determine the pressure values at points within the diffraction zone.

## 2. Methology

### *2.1 Assumptions*

To simplify the analysis, the following assumptions are adopted:

- Only shock wave propagation and its influencing factors are considered;

- The structure is treated as a perfectly rigid body, unaffected by the blast load;

- For surface-level explosions, the shock wave is assumed to propagate as a hemispherical front, and the impact of debris on the structure is neglected;

- The direction of shock wave propagation is perpendicular to the tunnel's cross-section.

Based on these assumptions, the following computational conditions are applied:

- Shock wave parameters are determined using empirical formulas for ground-level explosive charges;

- The shock wave propagates through air in a hemispherical pattern;

- Structural deformation and displacement resulting from shock wave interaction are not included in the analysis.

***2.2 Experimental formulas serving to calculate the propagating shock wave pressure value in the changing cross-section [1,2,3]***

When a bomb detonates at a distance $R_0$ from the road (Fig.1). At a point at a distance from the gate of the tunnel y, the over-pressure is calculated according to the following formula:

$$\Delta P_{\phi,y} = \alpha_1 \left[ \frac{6C}{R_0^2 (0.4R_0 + y)} + \sqrt[3]{\frac{C}{R_0^2 (0.4R_0 + y)}} \right] \quad (1)$$

there:

$R_0$ is the distance from the center of the explosion to tunnel gate (m);

C is the weight of explosive charge (kg);

$\Delta P_{\Phi,y}$: over-pressure at the calculation point (positive phase) (kG/cm²);

$\alpha_1$ is the factor that takes into account the effect of reflected pressure at the passageway:

+ if, $\Delta P_{\phi,R_0} = 100 (kG/cm^2)$ $\alpha_1 = 1.3$; $\Delta P_{\phi,R_0} = 1 (kG/cm^2)$ $\alpha_1 = 2$;

Other values of $\alpha_1$ are determined by interpolation;

+ if no reflection effect is taken into account, then $\alpha_1$=1;

y: Distance from the doorway to the measurement point (m).

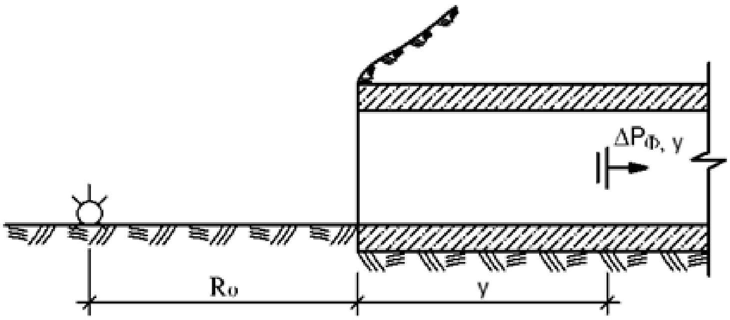


**Fig.1.***The Bomb exploded at $R_0$ road section*

*2.2.1 Propagation of the shock waves from narrow to large cross-sections [1,2,3]*

For scenarios involving an expanded cross-section (fig.2.a), as the shock wave propagates through the tunnel, the pressure value will decrease. This value can be determined by the formula (2):

$$\Delta P_{\phi,y*} = \alpha \cdot \Delta P_{\phi,y} \quad (2)$$

where $\alpha$ is the decline pressure coefficient:

$$\alpha = \left( \frac{S_1}{S_2} \right)^{0.8} \quad (3)$$

$S_1$ is the area of the narrow tunnel cross-section, m²;

$S_2$ is the area of the large tunnel cross-section, m²;

y*: Distance to form wave pressure in a variable cross-section (m).

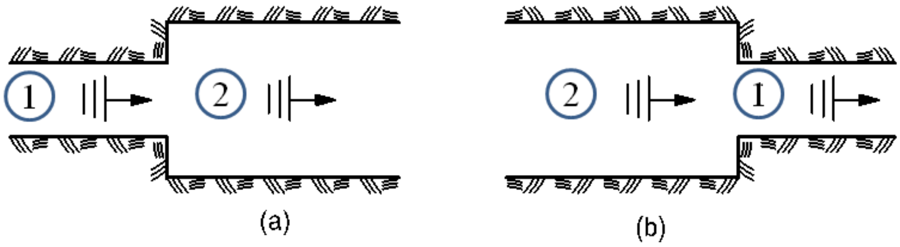


a) enlarged cross-section b) narrowed cross-section

**Fig.2.** *Propagation of shock waves in the tunnel with narrowed or enlarged cross-sections*

*2.2.2 Propagation of the shock waves from large sections to narrow sections [1,2,3]*

In the scenario involving a reduced cross-sectional area (Fig. 2.b), the propagation of the shock wave results in an increase in pressure, which is quantified by Equation (4):

$$\Delta P_{\phi,y*} = \beta \cdot \Delta P_{\phi,y} \quad (4)$$

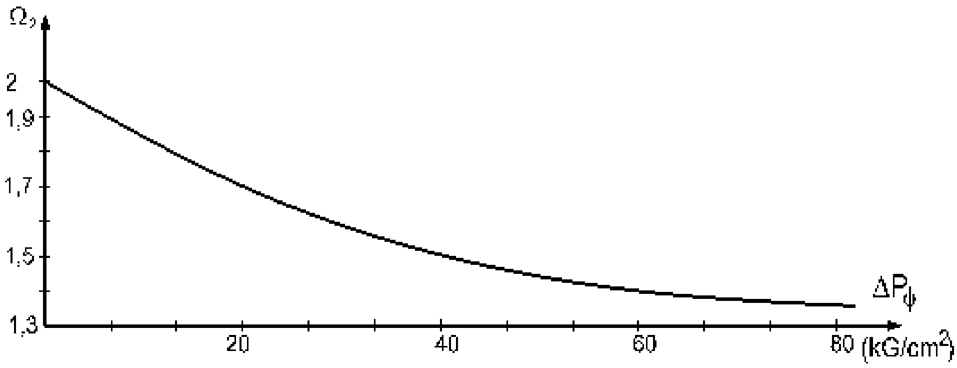


**Fig.3.** *Graph to determine frontal penetration coefficient* $\Omega_2$

in which the pressure increase coefficient $\beta$ is determined as follows:

If $d_2 \geq 2d_1$ is considered to be frontal penetration coefficient. Then $\beta = \Omega_2$;

in which $\Omega_2$ is the frontal penetration coefficient depending on the incident wave pressure $\Delta P_\Phi$, determined according to the graph in fig.3;

If $d_1 = d_2$ then clear $\beta = 1$;

If $d_1 < d_2 < 2d_1$. Value $\beta$ is interpolated between the above two cases;

$d_1$, $d_2$ are the equivalent diameters of tunnel cross-section 1 and 2 respectively;

y*: Distance to form wave pressure in a variable cross-section (m).

***2.3 Determining the shock wave pressure value propagating in a tunnel with variable cross-section by using software Ansys Autodyn3D***

*2.3.1 Material parameters*

This study investigates the impact of surface explosions located 15 meters from the tunnel gate, focusing on pressure propagation and structural response. The explosive charge: $C_{TNT}$ = 214 kg. The explosive charge is placed on the ground. Environment: Infinite air.

Atmospheric environment: use equation of state of ideal gas [4,5,6] as formula (5).

$$P = (\gamma - 1) \cdot \rho \cdot e \quad (5)$$

P - gas pressure (Pa); ρ - gas density (kg/m$^3$);

γ- ideal gas constant (kg/m$^3$); e - specific energy of the gas (J/kg.$^0$K).

**Table 1.** *The coefficients of the equation of the ideal gas state*

| ρ (kg/m$^3$) | γ (kg/m$^3$) | Temperature ($^0$K) | e (J/kg.$^0$K) |
|---|---|---|---|
| 1.225 | 1.4 | 288.200012 | 717.599976 |

Explosive products: use equation of state of explosive products Jones-Wilkens-Lee (abbreviated JWL) to calculate pressure values of explosion (p), this is semi-experimental equation [4,5,6]:

$$p = A\left(1-\frac{\omega}{R_1 V}\right)e^{-R_1 V} + B\left(1-\frac{\omega}{R_2 V}\right)e^{-R_2 V} + \frac{\omega \cdot E}{V} \quad (6)$$

there: the constants A, B, $R_1$, $R_2$, $\omega$ for TNT explosives are presented in Table 2; p is the pressure (kPa); $V=1/\rho_0$ is the specific volume; $\rho_0$ is the density of TNT explosives ($\rho_0$= 1630kg/m$^3$); E is energy per unit volume (E =6.0·10$^6$ kJ/m$^3$); explosion pressure $P_{CJ}$ = 2.1·10$^7$ (kPa); explosive speed: $v_{CJ}$ = 6930 (m/s).

**Table 2.** *Coefficients of the JWL equation of state*

| Explosive type | Coefficients of the JWL equation of state | | | | |
|---|---|---|---|---|---|
| | A (kPa) | B (kPa) | $R_1$ | $R_2$ | $\omega$ |
| TNT | 3.7377·10$^8$ | 3.7471·10$^6$ | 4.15 | 0.9 | 0.35 |

Tunnel: tunnel with cross-section (fig.4) be modelled in Ansys Autodyn3D as fig.5. Tunnel structure lining material is reinforced concrete with the strength of 35MPa.

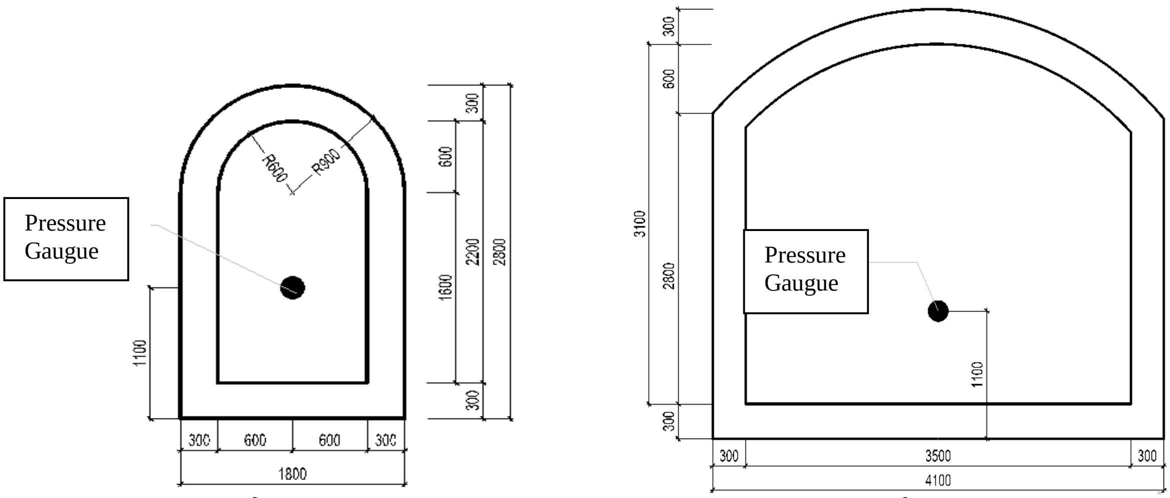


$S_1$ = 2.486 m$^2$; $d_1$ = 1.78 m    $S_2$ = 10.066 m$^2$; $d_2$ = 3.58 m

**Fig.4.** *Tunnel cross-section profiles*

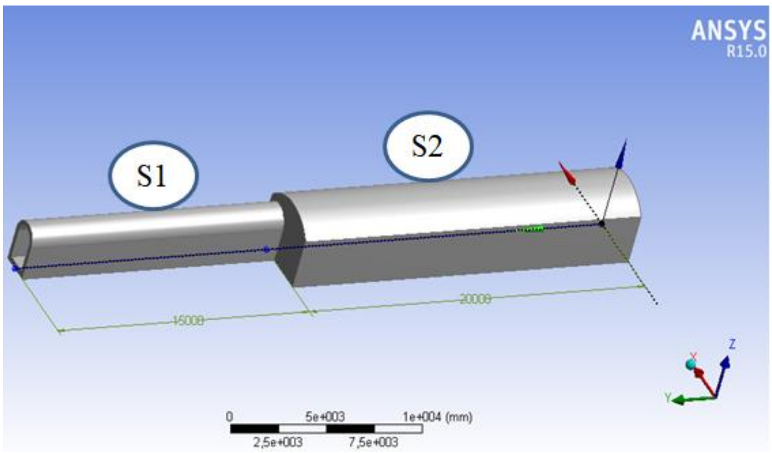


**Fig.5.** *Modelling in Ansys Autodyn3D*

*2.3.2 Procedure performed with Ansys 3D*

In this study, the geometric model consists of a 3D representation of a tunnel surrounded by infinite air, allowing for accurate modeling of shock wave behavior in an unbounded medium. Shock wave pressure values are calculated at various distances

(R) from the center of the TNT explosive charge. Given the significant element distortion expected during the simulation, an Arbitrary Lagrangian-Eulerian (ALE) mesh is adopted to leverage the strengths of both the Lagrangian and Eulerian approaches. The initial and boundary conditions are defined by excluding external influences on detonation and assuming a complete, stable explosion initiated at the center of the charge. The shock wave is propagated under the assumption of steady explosion velocity. Time steps and solution cycles are configured appropriately to ensure numerical stability. Following the simulation run, the results are post-processed and analyzed to evaluate shock wave pressure distribution and validate against reference data.

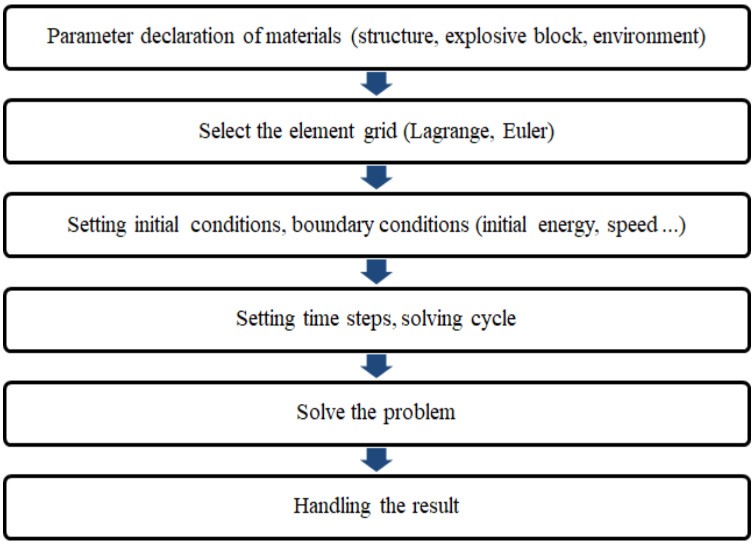


**Fig.6.** *Steps to solve the problem*

## 3. Numerical examples

### *3.1 The numerical example of shock waves propagating in enlarged tunnel cross-sections*

The arrangement of measurement points within the ANSYS Autodyn 3D simulation is illustrated in Figure 6.

The corresponding pressure values recorded at each measuring point are summarized as follows.

**Table 3.** *Summary of maximum pressure values at measurement points*

| Point | Coordinates (m) | | | $P_{max}$ (kPa) | Point | Coordinates (m) | | | $P_{max}$ (kPa) |
|---|---|---|---|---|---|---|---|---|---|
| | X | Y | Z | | | X | Y | Z | |
| 1 | 0 | 0 | 1.1 | 334.91 | 5 | -2.8 | 20 | 1.1 | 158.07 |
| 2 | 0 | 10 | 1.1 | 206.36 | 6 | -2.8 | 16 | 1.1 | 174.36 |
| 3 | 0 | 15 | 1.1 | 177.26 | 7 | -2.8 | 25 | 1.1 | 145.76 |
| 4 | 0 | 20 | 1.1 | 158.12 | 8 | 0 | 25 | 1.1 | 145.76 |

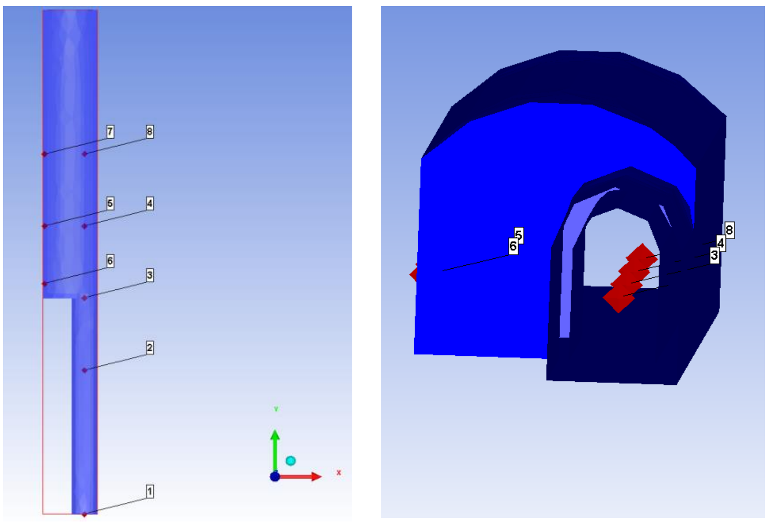

**Fig.7.** *Diagram of measuring point arrangement in Ansys Autodyn3D*

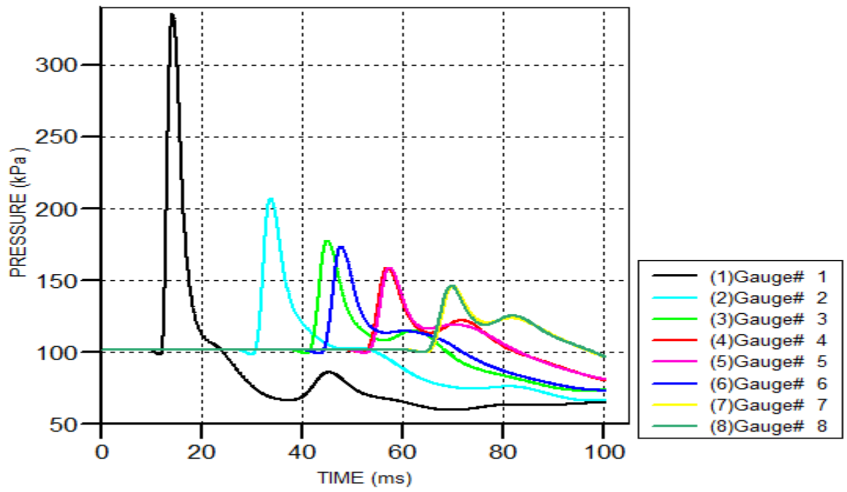


**Fig.8.** *Graph of pressure value at point 1; 2; 3; 4; 5; 6; 7; 8*

The simulation outcomes are compared against the results obtained using the experimental formulation. Shock wave pressure values within the tunnel are computed using Equation (1) at measurement points 1, 2, and 3. To enable direct comparison with the shock wave pressure values derived from the Ansys Autodyn3D simulation software, atmospheric pressure under standard conditions ($P_0$ = 101.325 kPa) is added to the calculated values. At points 7 and 8, where the tunnel cross-section transitions from narrow to wide, the pressure values are determined using Equations (2) and (3). The corresponding results are presented in Table 4.

**Table 4.** *Table comparing the results of pressure value in case of propagation from narrow to large cross-sections*

| Point | Geometry parameter | | | | Pressure Value | | | Notes |
|---|---|---|---|---|---|---|---|---|
| | Y (m) | $S_1$ ($m^2$) | $S_2$ ($m^2$) | $R_0$ (m) | Experimental formula (kPa) | Ansys (kPa) | Difference (%) | |
| 1 | 0 | | | 15 | 393.51 | 334.91 | 17.5 | tunnel head |
| 2 | 10 | | | 15 | 247.82 | 206.36 | 19.95 | |
| 3 | 15 | | | 15 | 224.54 | 177.26 | 26.67 | |
| 4 | 20 | | | 15 | | 158.12 | | y* <3$d_2$ diffraction region of wave (Lack of experiment formula) |
| 5 | 20 | 2.486 | 10.066 | 15 | | 158.07 | | y* <3$d_2$ diffraction region of wave (Lack of experiment formula) |
| 6 | 16 | 2.486 | 10.066 | 15 | | 174.36 | | y* <3$d_2$ diffraction region of wave (Lack of experiment formula) |
| 7 | 25 | 2.486 | 10.066 | 15 | 141.57 | 145.70 | -2.83 | y* > 3$d_2$ |
| 8 | 25 | 2.486 | 10.066 | 15 | 141.57 | 145.76 | -2.83 | y* > 3$d_2$ |

*Y: Distance from the doorway to the measuring point (m); y*: Distance to form wave pressure in a variable cross-section (m).*

Analysis of Table 4 reveals a decrease in simulated pressure values-observed from measuring points 3 to 8 when the tunnel cross-section transitions from narrow to wide. This trend aligns with the physical behavior of shock wave attenuation during expansion. The discrepancy between simulation results obtained from ANSYS Autodyn 3D and those calculated using empirical formulas ranges from 17.5% to 26.67%, which is considered acceptable for problems involving shock wave propagation. Notably, in the region inside the tunnel beyond $y^* > 3d_2$, this difference drops to under 2.83%, indicating strong agreement between both methods in more stable zones.

Furthermore, from the pressure graph at measuring points 3, 6, 4, and 5, the turbulent region-situated between $1.5d_2$ and $3d_2$—is clearly identifiable as the shock wave interacts with the geometric transition. This effect is particularly evident at points 4 and 5, located 5 meters downstream from the cross-sectional change, where pressure fluctuations reflect the wave's instability during its transition through varying geometry.

***3.2 The example of shock waves propagating in narrowed tunnel cross-sections***

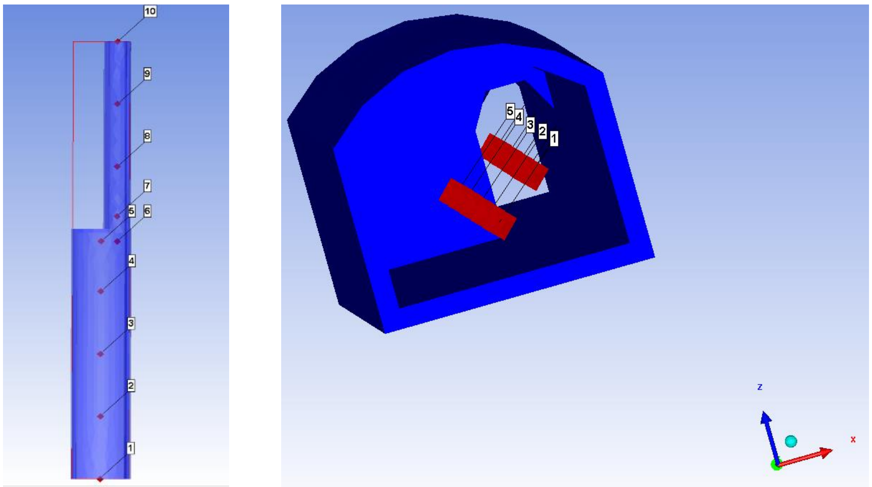


**Fig.9.** *Diagram of measuring point arrangement in Ansys Autodyn3D*

- Results of determination of pressure values at measuring points:

**Table 5.** *Summary of maximum pressure values at measuring points*

| Point | Coordinates (m) | | | $P_{max}$ (kPa) | Point | Coordinates (m) | | | $P_{max}$ (kPa) |
|---|---|---|---|---|---|---|---|---|---|
| | X | Y | Z | | | X | Y | Z | |
| 1 | 0 | 0 | 1.1 | 328.17 | 6 | 1.15 | 19 | 1.1 | 160.06 |
| 2 | 0 | 5 | 1.1 | 250.63 | 7 | 1.15 | 21 | 1.1 | 154.15 |
| 3 | 0 | 10 | 1.1 | 203.90 | 8 | 1.15 | 25 | 1.1 | 145.64 |
| 4 | 0 | 15 | 1.1 | 175.24 | 9 | 1.15 | 30 | 1.1 | 139.73 |
| 5 | 0 | 19 | 1.1 | 159.94 | 10 | 1.15 | 35 | 1.1 | 137.16 |

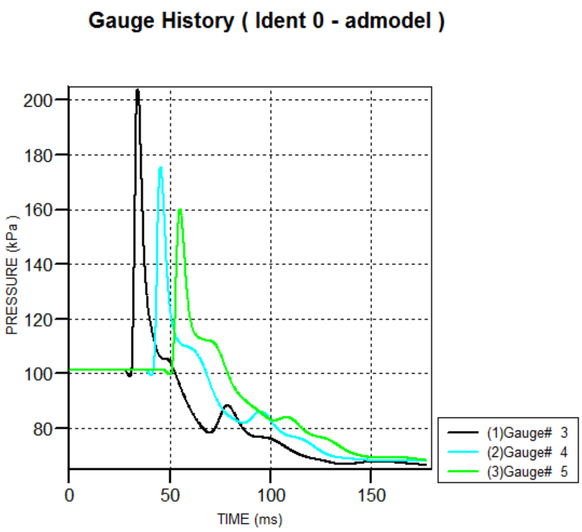


**Fig.10.** *Graph of pressure value at measuring points 3; 4; 5*

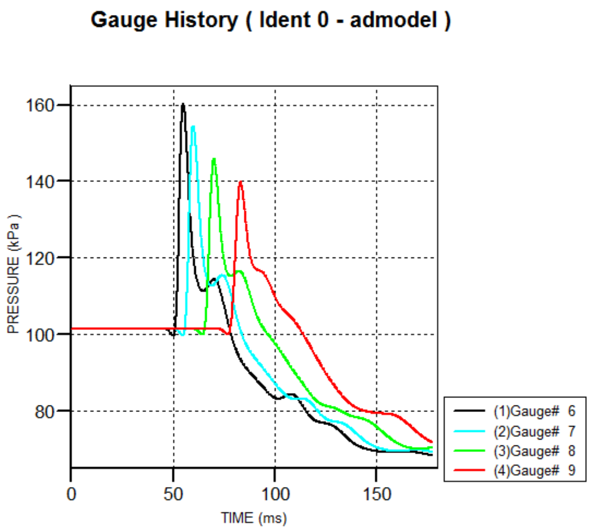


**Fig.11.** *Graph of pressure value at measuring points 6; 7; 8; 9.*

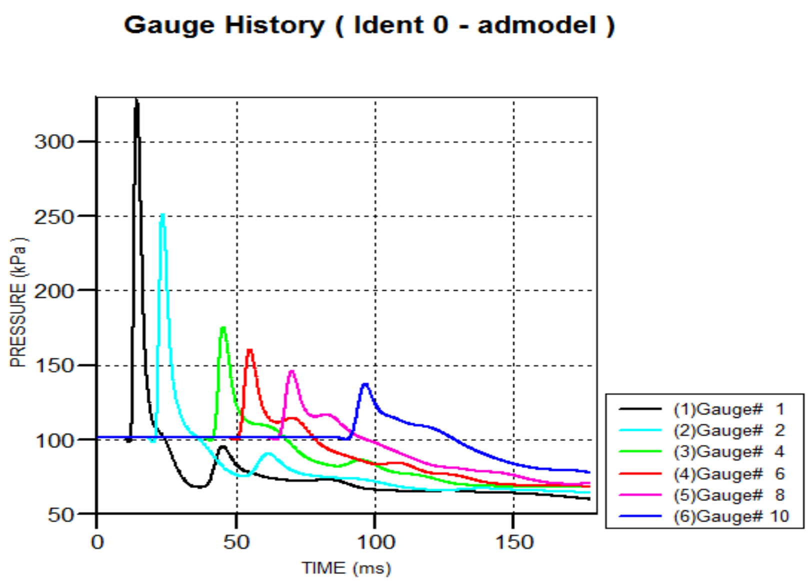


**Fig.12.** *Graph of pressure value at measuring point 1; 2; 4; 6; 8; 10*

- Results calculated according to the experimental formula (1) with measuring points 1; 2; 3; 4; 5; 6;

- Measuring point 9; 10. The pressure value when changing the cross-section from large to narrow is calculated by the formula (4). In our case, we have $d_2$= 3.58 m > $2d_1$ = 1.78·2 = 3.56 m. We have $d_2/d_1$ = 2.011. We have $\beta = \Omega_2$ = 1.995.

**Table 6.** *Table comparing the results of pressure values in case of of propagation from large to narrow cross-sections*

| Point | Geometry parameter | | | | Pressure Value | | | Notes |
|---|---|---|---|---|---|---|---|---|
| | Y (m) | $S_2$ ($m^2$) | $S_1$ ($m^2$) | $R_0$ (m) | Experimental formula (kPa) | Ansys (kPa) | Difference (%) | |
| 1 | 0 | | | 15 | 393.51 | 328.17 | 19.91 | tunnel head |
| 2 | 5 | | | 15 | 289.81 | 250.63 | 15.63 | |
| 3 | 10 | | | 15 | 247.82 | 203.90 | 21.54 | |
| 4 | 15 | | | 15 | 224.54 | 175.24 | 28.13 | |
| 5 | 19 | | | 15 | 212.06 | 159.94 | 32.59 | |
| 6 | 19 | | | 15 | 212.06 | 160.06 | 32.49 | |
| 7 | 21 | 10.066 | 2.486 | 15 | | 154.15 | | y* <$3d_1$ diffraction region of wave (Lack of experiment formula) |
| 8 | 25 | 10.066 | 2.486 | 15 | | 145.64 | | y* <$3d_1$ diffraction region of wave (Lack of experiment formula) |
| 9 | 30 | 10.066 | 2.486 | 15 | 185.60 | 139.73 | 32.83 | y* > $3d_1$ |
| 10 | 35 | 10.066 | 2.486 | 15 | 179.07 | 137.16 | 30.56 | y* > $3d_1$ |

*Y: Distance from the doorway to the measuring point (m); y*: Distance to form wave pressure in a variable cross-section (m).*

As the shock wave enters the tunnel from the outside, the pressure discrepancies between ANSYS Autodyn 3D simulation results and empirical formulas range from 15.63% to 32.83% across various measurement points. Despite this variation, the simulation outcomes remain consistent with the fundamental principles of shock wave propagation. In cases where the tunnel widens substantially ($d_2$ > $2d_1$) and the tunnel axis shifts at the cross-sectional transition, the pressure recorded at measurement point 6 (160.06 kPa) surpasses that at point 7 (154.15 kPa). This increase is attributed to the reflection of shock waves from the large, angled sidewalls, creating noticeable disturbances at points 5 and 6.

Further irregularities in the pressure readings at points 7 and 8—seen as fluctuations or "breaks" in the pressure curve—are caused by wave reflections from the tunnel walls and ceiling following the geometric change. These disturbances are most evident within the range of 1.5$d_1$ to 3$d_1$. Beyond this region, at measurement points 9 and 10 located 10 meters downstream (where 10 m > 3$d_1$ = 5.34 m), the reflected effects subside. The shock wave front becomes more uniform, and the pressure curve smoothens, indicating a return to stable, steady-state wave propagation.

### 4. Conclusion and discussion

This paper aims to investigate the pressure behavior of shock waves propagating through tunnels with cross-sectional variations, using ANSYS Autodyn 3D simulation software. The simulated results are compared with empirical formulas to assess their accuracy. Numerical testing reveals a discrepancy between simulation and experimental results ranging from 3% to 33%, a deviation considered acceptable for problems involving shock wave propagation.

Based on these findings, the study concludes that ANSYS Autodyn 3D provides a reliable method for determining shock wave pressure in tunnel environments. Furthermore, the software demonstrates potential for solving inverse problems and can serve as a valuable predictive tool for selecting appropriate explosive quantities prior to field testing.

**REFERENCES**

[1] *Bài giảng thiết kế kết cấu chống nổ* do Học viện Công trình Không quân Tây An biên soạn (1964).

[2] Đặng Văn Đích, Vũ Đình Lợi (1995), *Giáo trình công sự tập 1*, Học viện KTQS, Hà Nội.

[3] Nguyễn Trí Tá, Đặng Văn Đích, Vũ Đình Lợi (2008), *Giáo trình công sự tập 1*, Học viện KTQS, Hà Nội.

[4] AUTODYN help (2009), ANSYS WORKBENCH 14.5.

[5] B, M, Dobratz; P, C, Crawford (1985), *"LLNL Explosives Handbook: Properties of Chemical Explosives and Explosive Simulants"*, Ucrl-52997, Retrieved 31 August 2018.

[6] E. Lee, M. Finger, W. Collins (1973), *JWL equations of state coefficient for high explosives*, Lawrence Livermore Laboratory, Livermore, Calif, UCID-16189, Berkeley.

[7] Баум Ф,А,, иОрленко Л, П, (2002), *"Физика взрывка"*, tom1, Москва.

[8] D.J. Benson (1992). *Computational methods in Lagrangian and Eulerian hydrocodes*. Computer methods in Applied mechanics and Engineering. 99, 235-394.

[9] J. Donea (1983). *Arbitrary Lagrangian-Eulerian finite element analysis*. Computational methods for transient analysis. 474-516.

[10] M.A. Puso, J. Sanders, R. Settgast, B. Liu (2012). *An embedded mesh method in a multiple material ALE*. Computer Methods in Applied Mechanics and Engineering. 245, 273-289.

[11] Y.-T. Wang, J.-Z. Zhang (2011). *An improved ALE and CBS-based finite element algorithm for analyzing flows around forced oscillating bodies*. Finite Elements in Analysis and Design. 47, 1058-1065.